SIAM J. SCI. COMPUT.
Vol. 36, No. 4, pp. A1797–A1812

A CHEBYSHEV PSEUDOSPECTRAL METHOD TO SOLVE THE SPACE-TIME TEMPERED FRACTIONAL DIFFUSION EQUATION*

EMMANUEL HANERT† AND CÉCILE PIRET‡

Abstract. The tempered fractional diffusion equation is a generalization of the standard fractional diffusion equation that includes the truncation effects inherent to finite-size physical domains. As such, that equation better describes anomalous transport processes occurring in realistic complex systems. To broaden the range of applicability of tempered fractional diffusion models, efficient numerical methods are needed to solve the model equation. In this work, we have developed a pseudospectral scheme to discretize the space-time fractional diffusion equation with exponential tempering in both space and time. The model solution is expanded in both space and time in terms of Chebyshev polynomials and the discrete equations are obtained with the Galerkin method. Numerical examples are provided to highlight the convergence rate and the flexibility of this approach. The proposed Chebyshev pseudospectral method yields an exponential rate of convergence when the solution is smooth and allows a great flexibility to simultaneously handle fractional time and space derivatives with different levels of truncation. Our results confirm that nonlocal numerical methods are best suited to discretize fractional differential equations as they naturally take the global behavior of the solution into account.

Key words. fractional derivatives, anomalous diffusion, exponentially truncated power laws, pseudospectral method

AMS subject classifications. 35R11, 65N35

DOI. 10.1137/130927292

1. Introduction.

Anomalous diffusion models provide a better description of transport processes taking place in complex heterogeneous systems (see, for instance, [27, 28, 2] and the references therein). These models rely on fractional-order derivatives to represent the observed superlinear or sublinear growth of the variance of the variable of interest. The former corresponds to superdiffusion and the latter to subdiffusion. Superdiffusion is typically characterized by spatially nonlocal transport (i.e., large displacements) and modeled by a fractional diffusion term. Subdiffusion is characterized by temporally nonlocal transport (i.e., memory effects) and modeled by a fractional time derivative. Anomalous diffusion models are the fluid limit of a continuous time random walk with a heavy-tailed power-law probability distribution function (PDF) for both the displacements and the waiting times. The slow power-law decay of these distributions leads to diverging moments in both space and time, which can be problematic from a physical point of view. Indeed, for most practical applications, there are upper bounds on the displacements that a particle can make or on the waiting times between these displacements. These upper bounds should thus be taken into account by the model.

One way to recover finite moments is to truncate the displacements and waiting time PDFs beyond a certain threshold corresponding to the limits of the physical system. Truncated Lévy processes were first introduced by Mantegna and Stanley

*Submitted to the journal's Methods and Algorithms for Scientific Computing section July 1, 2013; accepted for publication (in revised form) May 14, 2014; published electronically August 12, 2014.

http://www.siam.org/journals/sisc/36-4/92729.html

†Université catholique de Louvain, Earth and Life Institute (ELI), Croix du Sud 2 box L7.05.16, B-1348 Louvain-la-Neuve, Belgium (emmanuel.hanert@uclouvain.be).

‡Université catholique de Louvain, Institute of Mechanics, Materials and Civil Engineering (iMMC), 4 Avenue G. Lemaître, B-1348 Louvain-la-Neuve, Belgium (cecile.piret@uclouvain.be).

[23] and Koponen [16] to eliminate arbitrarily large displacements. Exponentially tempered Lévy processes were proposed by Rosiński [36] as a smoother alternative. In that case, the sharp cutoff is replaced by a smooth exponential damping of the tails of the displacement PDF. Exponentially tempered Lévy processes lead to a tempered fractional diffusion equation in the fluid limit [5, 1]. Following the same approach, the waiting times between particle displacements can be tempered as well. In the fluid limits, it leads to a fractional diffusion equation with a tempered time derivative [26]. By tempering displacement and waiting time PDFs, one obtains a space-time tempered fractional diffusion equation that yields convergent moments in both space and time [43] and whose dynamics ultimately converges to normal diffusion [5, 26]. Tempering therefore modifies the dynamics of systems driven by anomalous diffusion [8, 18] and appears to be better suited for practical applications [6, 44].

The application of tempered fractional diffusion models to realistic problems strongly depends on the numerical schemes available to solve the model equation. So far, Lagrangian particle tracking methods and Eulerian finite difference (FD) schemes have been proposed to solve that equation [26, 1, 45]. Here, we will not consider Lagrangian methods but only focus on Eulerian ones. The FD scheme of [26, 1, 45] is an extension of the scheme proposed by [24, 25, 37] to discretize the fractional diffusion operator without tempering. The same approach can be used to discretize the fractional time derivative [22, 33, 7]. Some numerical schemes using low-order finite elements (FE) have also been proposed [11, 35, 14] to discretize the fractional diffusion term without tempering. Since fractional derivatives are nonlocal operators, FD and FE schemes generate large, full coefficient matrices. They require a computational cost of $\mathcal{O}(n^3)$ and storage of $\mathcal{O}(n^2)$, where n is the number of degrees of freedom. To reduce the computational burden, Wang and others recently proposed a fast FD method based on the method of [24, 25] that only requires a storage of $\mathcal{O}(n)$ and a computational cost of $\mathcal{O}(n \log^2 n)$ [40, 39]. The computational cost has been further reduced by Pang and Sun, who achieved $\mathcal{O}(n \log n)$ by using a multigrid method [29].

Another approach to design an efficient numerical scheme is to discretize these nonlocal differential operators with nonlocal numerical methods. Hence, the global behavior of the solution can be naturally taken into account and the computational cost is not substantially increased when moving from a second-order to a fractional-order diffusion model. Following that approach, pseudospectral (PS) methods based on expansions of the model solution in terms of Chebyshev, Jacobi, or Mittag–Leffler basis functions have been proposed to discretize the space and/or time fractional diffusion equation [21, 12, 13, 9, 10, 20, 4, 41]. With these methods, the discrete equations can be derived by using either collocation, tau or Galerkin methods. The radial basis function has also recently been used to discretize the space-fractional diffusion equation [30]. All these methods offer spectral accuracy, meaning that the error decreases exponentially fast as the number of nodes increases.

In this paper, we present a high-order numerical discretization of the space-time fractional diffusion equation with exponential tempering in both space and time. The PS numerical scheme is based on a space-time expansion of the model solution in terms of Chebyshev polynomials. Such a discretization is exponentially accurate in both space and time when the solution is smooth and takes full advantage of the nonlocal nature of fractional differential operators. Numerical examples are provided to highlight the convergence of the method for both smooth and nonsmooth solutions as well as its ability to handle steep initial conditions and generic boundary conditions.

2. Mathematical model. We consider a general diffusion equation that combines the tempered space and time fractional diffusion equations. The tempered time fractional equation was originally proposed by Meerschaert, Zhang, and Baeumer [26] to represent the dynamics of a tracer in the mobile phase, while the tempered fractional diffusion operator in space was introduced by Cartea and del Castillo Negrete [5]. The model equation reads

$$\partial_t^{\gamma,\beta,s} f(x,t) = d(x,t)\ \partial_x^{\alpha,\theta,\lambda} f(x,t) + q(x,t), \tag{2.1}$$

where the functions $d(x,t) > 0$ and $q(x,t)$ are a generalized diffusivity term (SI units: $\mathrm{m}^{\alpha}\mathrm{s}^{-1}$) and a reaction term, respectively. The operator on the left-hand side of (2.1) is a tempered fractional derivative of order γ defined as

$$\partial_t^{\gamma,\beta,s} f(x,t) = \frac{\partial f}{\partial t}(x,t) + \beta e^{-st}\,{}_0D_t^{\gamma}\left(e^{st} f(x,t)\right) - \beta s^{\gamma} f(x,t), \tag{2.2}$$

where β is a capacity coefficient of SI units $\mathrm{s}^{\gamma-1}$, and $s \geq 0$ is the time truncation parameter (SI units: s^{-1}). The operator on the right-hand side of (2.1) is a tempered diffusion operator of order α defined as

$$\begin{aligned}\partial_x^{\alpha,\theta,\lambda} f(x,t) = {} & \frac{1-\theta}{2} e^{-\lambda x}\,{}_0D_x^{\alpha}\left(e^{\lambda x} f(x,t)\right) + \frac{1+\theta}{2} e^{\lambda x}\,{}_xD_L^{\alpha}\left(e^{-\lambda x} f(x,t)\right) \\ & - \lambda^{\alpha} f(x,t) + \alpha\theta\lambda^{\alpha-1}\frac{\partial f}{\partial x}(x,t),\end{aligned} \tag{2.3}$$

where $\lambda \geq 0$ is the space truncation parameter whose SI units are m^{-1}, and $\theta \in [-1,1]$ is a skewness parameter. Equation (2.1) is solved for $0 \leq x \leq L$ and $0 \leq t \leq T$.

The fractional-order derivatives appearing in (2.2) and (2.3) can be defined in the Riemann–Liouville or Caputo sense. Unlike Riemann–Liouville derivatives, Caputo derivatives are not singular on the domain boundaries. That feature makes them particularly appealing for nonlocal numerical methods, like the PS method, as most basis functions take a nonzero value on the boundary. Zhang et al. have also shown that Riemann–Liouville derivatives could cause mass-balance errors on bounded domains [42]. The time and space derivatives are thus defined in the Caputo sense as follows:

$$\begin{aligned}{}_0D_t^{\gamma} u(t) &= \frac{1}{\Gamma(1-\gamma)}\int_0^t \frac{\frac{\partial u(\tau)}{\partial \tau}}{(t-\tau)^{\gamma}}\,\mathrm{d}\tau, \\ {}_0D_x^{\alpha} v(x) &= \frac{1}{\Gamma(2-\alpha)}\int_0^x \frac{\frac{\partial^2 v(y)}{\partial y^2}}{(x-y)^{\alpha-1}}\,\mathrm{d}y, \\ {}_xD_L^{\alpha} v(x) &= \frac{1}{\Gamma(2-\alpha)}\int_x^L \frac{\frac{\partial^2 v(y)}{\partial y^2}}{(y-x)^{\alpha-1}}\,\mathrm{d}y,\end{aligned}$$

where $\Gamma(.)$ is Euler's gamma function. For simplicity, we have assumed that $1 < \alpha \leq 2$ and $0 < \gamma \leq 1$. It should be noted that the weighting factors in front of the left and right space derivatives are slightly different from the ones used by [5].

Initial and boundary conditions also have to be specified to solve (2.1). Here, we consider an arbitrary initial condition of the form $f(x,0) = f^0(x)$, where f^0 is a given function defined on $[0,L]$. The specification of boundary conditions is a more delicate issue. Most studies dealing with the numerical solution of the fractional diffusion equation on a bounded domain simply use the same boundary conditions as the one

used for the classical diffusion equation. That is the approach we have chosen to follow in this work. We therefore consider the following Robin boundary conditions:

$$c_d^l f(0,t) + c_n^l \frac{\partial f}{\partial x}(0,t) = f^l(t),$$
$$c_d^r f(L,t) + c_n^r \frac{\partial f}{\partial x}(L,t) = f^r(t).$$

The coefficients $c_d^l, c_n^l, c_d^r,$ and c_n^r allow us to specify either the value of the solution, the value of its slope or a combination of both on the boundaries. The functions f^l and f^r are given functions defined on $[0,T]$.

The boundary conditions that we impose are mathematically sound and numerically stable but unfortunately not always physically realistic. The lack of physical realism is due to the nonlocal nature of the anomalous diffusion flux. Hence, fixing the slope of the solution on the boundary does not determine that flux. A homogeneous Neumann boundary condition would therefore neither guarantee mass conservation nor effectively yield a zero slope on the boundary. A very recent study by Kay et al. [15] shows how to impose physically plausible reflecting boundary conditions for anomalous diffusion models on bounded domains. This work builds upon the work of Krepysheva, Di Pietro, and Neel [17], who considered reflecting boundary conditions at $x = 0$ on a semi-infinite domain. By expressing the model in terms of a Lévy random walk and the generalized master equation, Kay et al. [15] derived a modified kernel for the Riesz fractional derivative for a finite domain $[0, L]$ with two reflecting boundary conditions. For such a domain, the jump of a particle from a point x to x' can be obtained in infinitely many ways via repeated bounces from the two walls. The resulting continuous model then involves a Riesz fractional diffusion operator defined on $\mathbb{R}$ acting on the periodic triangular function extension to $\mathbb{R}$ of the model solution $f(x,t)$ defined on $[0,L]$. In their work, Kay et al. also propose an FD and a finite volume scheme to approximate this operator by applying a finite set of reflections. They show that total mass is increasingly conserved with reflecting boundary conditions as the number of reflections increases. Furthermore, the gradient of the solution approaches zero as the number of reflections increases.

Applying such boundary conditions to a PS scheme has never been done before and is not straightforward. We therefore prefer to leave that extension to a future study and focus here on the numerical solution of a fully tempered fractional diffusion equation with classical boundary conditions.

3. PS numerical discretization. In this section, we derive a space-time discretization of (2.1) based on the Galerkin method with Chebyshev expansions in both space and time. The discrete solution is expressed in terms of a matrix of unknown coefficients F_{jk} as follows:

$$f(x,t) \approx \tilde{f}(x,t) = \sum_{j=0}^{N_x} \sum_{k=0}^{N_t} \phi_j^x(x) \mathsf{F}_{jk} \phi_k^t(t), \tag{3.1}$$

where

$$\phi_j^x(x) = \phi_j(\xi(x)) \qquad \text{for } j = 0, \ldots, N_x,$$
$$\phi_k^t(t) = \phi_k(\tau(t)) \qquad \text{for } k = 0, \ldots, N_t,$$

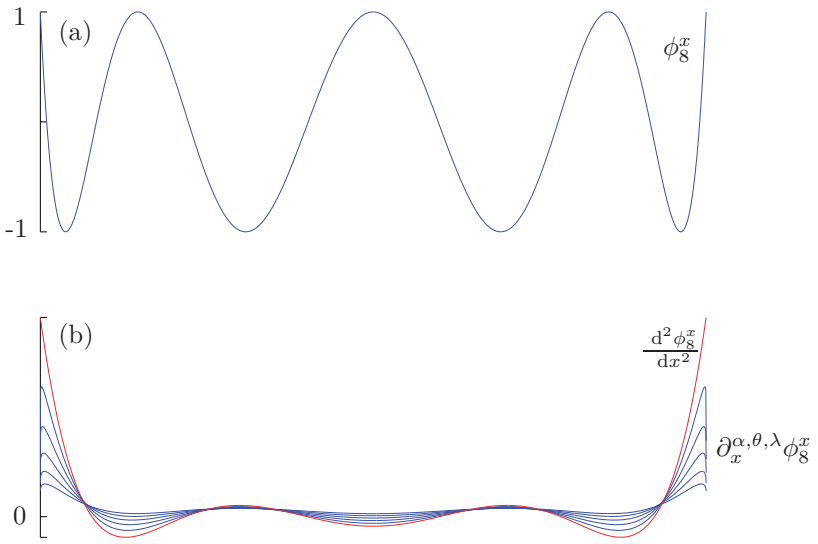

FIG. 1. *Example of* (a) *the eighth-order Chebyshev PS basis function* ϕ_8^x*, and* (b) *the second-order derivative* ($\frac{d^2\phi_8^x}{dx^2}$*, in red) and the fractional-order derivatives* ($\partial_x^{\alpha,\theta,\lambda}\phi_8^x$*, in blue) of* ϕ_8^x *for* $\alpha = 1.5, 1.6, 1.7, 1.8, 1.9$*,* $\theta = 0$*, and* $\lambda = 0$*. Note that* ϕ_8^x*,* $\frac{d^2\phi_8^x}{dx^2}$*, and all the fractional derivatives are global functions.*

and ϕ_j and ϕ_k are the Chebyshev polynomials of order j and k defined on $[-1, 1]$. The functions $\xi : x \in [0, L] \mapsto \frac{2x}{L} - 1$ and $\tau : t \in [0, T] \mapsto \frac{2t}{T} - 1$ are isomorphisms that map the physical domain $[0, L] \times [0, T]$ to the computational domain $[-1, 1] \times [-1, 1]$. By using an expansion in terms of Chebyshev polynomials, the PS method naturally takes the global behavior of the solution into account, in both space and time. This is advantageous for fractional-order models as the computational cost of the method is not substantially increased when replacing integer-order derivatives by fractional-order ones. As an illustration, Figure 1 shows the basis function $\phi_8^x(x)$ and its derivatives, which are all smooth global functions. The basis functions being polynomials, their fractional derivatives can be computed analytically (see, for instance, [31, 20]).

Before deriving the discrete equations, we will assume that the diffusivity is a separable function and that it can thus be expressed as the product of two functions depending on only one variable, i.e., $d(x, t) = d^x(x)d^t(t)$. This is not a strong assumption as for most applications the diffusivity does not depend on time. We shall also introduce the following three intermediate variables and assume that they have the same discretization as the model solution:

$$g(x,t) \equiv e^{st} f(x,t) \approx \tilde{g}(x,t) = \sum_{j=0}^{N_x} \sum_{k=0}^{N_t} \phi_j^x(x) \mathsf{G}_{jk} \phi_k^t(t),$$

$$h^l(x,t) \equiv e^{\lambda x} f(x,t) \approx \tilde{h}^l(x,t) = \sum_{j=0}^{N_x} \sum_{k=0}^{N_t} \phi_j^x(x) \mathsf{H}^l_{jk} \phi_k^t(t),$$

$$h^r(x,t) \equiv e^{-\lambda x} f(x,t) \approx \tilde{h}^r(x,t) = \sum_{j=0}^{N_x} \sum_{k=0}^{N_t} \phi_j^x(x) \mathsf{H}^r_{jk} \phi_k^t(t),$$

where G, H^l, and H^r are the corresponding coefficient matrices that define the Chebyshev expansions. Finally, we introduce the following notation for the integrals involved in the Galerkin formulation of the model equations:

$$\begin{aligned}\langle\!\langle\cdot\rangle\!\rangle &\equiv \int_0^L\int_0^T \cdot\, w(\xi(x))w(\tau(t))\ \mathrm{d}x\ \mathrm{d}t,\\ \langle\cdot\rangle_x &\equiv \int_0^L \cdot\, w(\xi(x))\ \mathrm{d}x,\\ \langle\cdot\rangle_t &\equiv \int_0^T \cdot\, w(\tau(t))\ \mathrm{d}t,\end{aligned}$$

where $w : y \in [-1,1] \mapsto \frac{1}{\sqrt{1-y^2}}$ is the weight function associated with Chebyshev polynomials.

A PS discretization of (2.1) based on the Galerkin method is obtained by introducing the discrete variables in (2.1) and orthogonalizing the residual with respect to the set of basis functions. The following discrete equations are then obtained:

$$\langle\!\langle \phi_i^x \partial_t^{\gamma,\beta,s}\tilde{f}(x,t)\phi_l^t\rangle\!\rangle = \langle\!\langle \phi_i^x d(x,t)\partial_x^{\alpha,\theta,\lambda}\tilde{f}(x,t)\phi_l^t\rangle\!\rangle + \langle\!\langle \phi_i^x q(x,t)\phi_l^t\rangle\!\rangle \tag{3.2}$$

for $0 \le i \le N_x$ and $0 \le l \le N_t$. In the remainder of the derivation, we shall always assume that the indices i and j vary between 0 and N_x and that the indices k and l vary between 0 and N_t. We shall also assume that a repeated index is summed over.

Let us first consider the discretization of the fractional time derivative and express it in matrix form:

$$\begin{aligned}&\langle\!\langle \phi_i^x \partial_t^{\gamma,\beta,s}\tilde{f}\phi_l^t\rangle\!\rangle\\ &\quad= \left\langle\!\!\left\langle \phi_i^x \frac{\partial\tilde{f}}{\partial t}\phi_l^t\right\rangle\!\!\right\rangle + \beta\langle\!\langle \phi_i^x e^{-st}{}_0D_t^\gamma\tilde{g}\ \phi_l^t\rangle\!\rangle - \beta s^\gamma\langle\!\langle \phi_i^x\tilde{f}\phi_l^t\rangle\!\rangle\\ &\quad= \langle\phi_i^x\phi_j^x\rangle_x\ \mathsf{F}_{jk}\left\langle\frac{\mathrm{d}\phi_k^t}{\mathrm{d}t}\phi_l^t\right\rangle + \beta\langle\phi_i^x\phi_j^x\rangle_x\ \mathsf{G}_{jk}\ \langle e^{-st}{}_0D_t^\gamma\phi_k^t\ \phi_l^t\rangle_t\\ &\qquad- \beta s^\gamma\langle\phi_i^x\phi_j^x\rangle_x\ \mathsf{F}_{jk}\ \langle\phi_k^t\phi_l^t\rangle_t\\ &\quad= \mathsf{M}_{ij}\mathsf{F}_{jk}\mathsf{T}^1_{kl} + \beta\ \mathsf{M}_{ij}\mathsf{G}_{jk}\mathsf{T}^\gamma_{kl} - \beta s^\gamma\ \mathsf{M}_{ij}\mathsf{F}_{jk}\mathsf{N}_{kl},\end{aligned}$$

where we have introduced the matrices M, T^1, T^γ, and N whose entries are defined as

$$\mathsf{M}_{ij} \equiv \langle\phi_i^x\phi_j^x\rangle_x\ ,\quad \mathsf{T}^1_{kl} \equiv \left\langle\frac{\mathrm{d}\phi_k^t}{\mathrm{d}t}\phi_l^t\right\rangle,\quad \mathsf{T}^\gamma_{kl} \equiv\ \langle e^{-st}{}_0D_t^\gamma\phi_k^t\phi_l^t\rangle_t,\quad \mathsf{N}_{kl} \equiv\ \langle\phi_k^t\phi_l^t\rangle_t.$$

All these integrals can be computed to essentially machine precision with a Gauss–Chebyshev quadrature.

The last step to obtain a tractable discretization of the fractional derivative is to express the matrix G in terms of F. This can be done by using the L_2 projection

$$\langle\!\langle \phi_i^x\tilde{g}(x,t)\phi_l^t\rangle\!\rangle = \langle\!\langle \phi_i^x e^{st}\tilde{f}(x,t)\phi_l^t\rangle\!\rangle$$

or

$$\langle\phi_i^x\phi_j^x\rangle_x\ \mathsf{G}_{jk}\ \langle\phi_k^t\phi_l^t\rangle_t = \langle\phi_i^x\phi_j^x\rangle_x\ \mathsf{F}_{jk}\ \langle e^{st}\phi_k^t\phi_l^t\rangle_t,$$

which amounts to saying that $\mathsf{G} = \mathsf{F}\mathsf{E}^p\mathsf{N}^{-1}$, where the matrix E^p is such that $\mathsf{E}^p_{kl} = \langle e^{st}\phi^t_k\phi^t_l\rangle_t$. The PS Galerkin discretization of the tempered fractional derivative can then be expressed in shorthand notation as a product of three matrices:

$$\langle\!\langle \phi^x_i \partial_t^{\gamma,\beta,s}\tilde{f}(x,t)\phi^t_l\rangle\!\rangle = (\mathsf{MFT})_{il}\,,$$

where

$$\mathsf{T} \equiv \mathsf{T}^1 + \beta\ \mathsf{E}^p\mathsf{N}^{-1}\mathsf{T}^\gamma - \beta s^\gamma\ \mathsf{N}. \tag{3.3}$$

It should be noted that the classical time-fractional diffusion model without tempering can easily be included within this framework. In that case, the time derivative is simply $\partial_t^{\gamma,\beta,s} f = {}_0D_t^\gamma f$ and the entries of matrix T must then be defined as $\mathsf{T}_{kl} = \langle {}_0D_t^\gamma \phi^t_k\phi^t_l\rangle_t$.

The discretization of the fractional diffusion term with the Galerkin method is similar. It can be summarized as follows:

$$\begin{aligned}
&\langle\!\langle \phi^x_i d\ \partial_x^{\alpha,\theta,\lambda}\tilde{f}\phi^t_l\rangle\!\rangle \\
&\quad= \frac{1-\theta}{2}\langle\!\langle \phi^x_i d\ e^{-\lambda x}{}_0D_x^\alpha\tilde{h}^l\ \phi^t_l\rangle\!\rangle + \frac{1+\theta}{2}\langle\!\langle \phi^x_i d\ e^{\lambda x}{}_xD_L^\alpha\tilde{h}^r\ \phi^t_l\rangle\!\rangle \\
&\qquad- \lambda^\alpha\langle\!\langle \phi^x_i d\ \tilde{f}\phi^t_l\rangle\!\rangle + \alpha\theta\lambda^{\alpha-1}\left\langle\!\!\left\langle \phi^x_i d\ \frac{\partial\tilde{f}}{\partial x}\phi^t_l\right\rangle\!\!\right\rangle, \\
&\quad= \frac{1-\theta}{2}\langle\phi^x_i d^x e^{-\lambda x}{}_0D_x^\alpha\phi^x_j\rangle_x\ \mathsf{H}^l_{jk}\ \langle\phi^t_k d^t\phi^t_l\rangle_t + \frac{1+\theta}{2}\langle\phi^x_i d^x e^{\lambda x}{}_xD_L^\alpha\phi^x_j\rangle_x\ \mathsf{H}^r_{jk}\ \langle\phi^t_k d^t\phi^t_l\rangle_t \\
&\qquad- \lambda^\alpha\langle\phi^x_i d^x\phi^x_j\rangle_x\ \mathsf{F}_{jk}\ \langle\phi^t_k d^t\phi^t_l\rangle_t + \alpha\theta\lambda^{\alpha-1}\left\langle \phi^x_i d^x\frac{\mathrm{d}\phi^x_j}{\mathrm{d}x}\right\rangle\mathsf{F}_{jk}\ \langle\phi^t_k d^t\phi^t_l\rangle_t \\
&\quad= \mathsf{D}^l_{ij}\mathsf{H}^l_{jk}\mathsf{P}_{kl} + \mathsf{D}^r_{ij}\mathsf{H}^r_{jk}\mathsf{P}_{kl} - \mathsf{R}_{ij}\mathsf{F}_{jk}\mathsf{P}_{kl} + \mathsf{A}_{ij}\mathsf{F}_{jk}\mathsf{P}_{kl},
\end{aligned}$$

where the entries of the matrices D^l, D^r, P, R, and A are defined as

$$\begin{aligned}
&\mathsf{D}^l_{ij} \equiv \frac{1-\theta}{2}\langle\phi^x_i d^x e^{-\lambda x}{}_0D_x^\alpha\phi^x_j\rangle_x\ , && \mathsf{D}^r_{ij} \equiv \frac{1+\theta}{2}\langle\phi^x_i d^x e^{\lambda x}{}_xD_L^\alpha\phi^x_j\rangle_x\ , \\
&\mathsf{R}_{ij} \equiv \lambda^\alpha\langle\phi^x_i d^x\phi^x_j\rangle_x\ , && \mathsf{A}_{ij} \equiv \alpha\theta\lambda^{\alpha-1}\left\langle \phi^x_i d^x\frac{\mathrm{d}\phi^x_j}{\mathrm{d}x}\right\rangle, \\
&\mathsf{P}_{kl} \equiv\ \langle\phi^t_k d^t\phi^t_l\rangle_t.
\end{aligned}$$

It should be noted that integration by parts could be used to compute D^l_{ij} and D^r_{ij}. Doing so would introduce boundary terms depending on a fractional-order flux. That flux could then be specified weakly on the boundaries.

As for the discretization of the time derivative, we still have to express the auxiliary variables H^l and H^r in terms of F. This is again done with an L_2 projection,

$$\begin{aligned}
\langle\!\langle \phi^x_i\tilde{h}^l(x,t)\phi^t_l\rangle\!\rangle &= \langle\!\langle \phi^x_i e^{\lambda x}\tilde{f}(x,t)\phi^t_l\rangle\!\rangle, \\
\langle\!\langle \phi^x_i\tilde{h}^r(x,t)\phi^t_l\rangle\!\rangle &= \langle\!\langle \phi^x_i e^{-\lambda x}\tilde{f}(x,t)\phi^t_l\rangle\!\rangle,
\end{aligned}$$

which can be rewritten as

$$\begin{aligned}
\langle\phi^x_i\phi^x_j\rangle_x\ \mathsf{H}^l_{jk}\ \langle\phi^t_k\phi^t_l\rangle_t &= \langle\phi^x_i e^{\lambda x}\phi^x_j\rangle_x\ \mathsf{F}_{jk}\ \langle\phi^t_k\phi^t_l\rangle_t, \\
\langle\phi^x_i\phi^x_j\rangle_x\ \mathsf{H}^r_{jk}\ \langle\phi^t_k\phi^t_l\rangle_t &= \langle\phi^x_i e^{-\lambda x}\phi^x_j\rangle_x\ \mathsf{F}_{jk}\ \langle\phi^t_k\phi^t_l\rangle_t.
\end{aligned}$$

Introducing the matrices E^l and E^r whose entries are $\mathsf{E}^l_{ij} = \langle \phi_i^x e^{\lambda x} \phi_j^x \rangle_x$ and $\mathsf{E}^r_{ij} = \langle \phi_i^x e^{-\lambda x} \phi_j^x \rangle_x$, we easily see that $\mathsf{H}^l = \mathsf{M}^{-1}\mathsf{E}^l\mathsf{F}$ and $\mathsf{H}^r = \mathsf{M}^{-1}\mathsf{E}^r\mathsf{F}$.

The PS Galerkin discretization of the tempered fractional diffusion term can then be expressed by the product of three matrices:

$$\langle\!\langle \phi_i^x d(x,t) \partial_x^{\alpha,\theta,\lambda} \tilde{f}(x,t) \phi_l^t \rangle\!\rangle = (\mathsf{DFP})_{il},$$

where

$$\mathsf{D} \equiv \mathsf{D}^l\mathsf{M}^{-1}\mathsf{E}^l + \mathsf{D}^r\mathsf{M}^{-1}\mathsf{E}^r - \mathsf{R} + \mathsf{A}. \tag{3.4}$$

It is important to note that M and N are diagonal matrices thanks to the orthogonality of Chebyshev polynomials. Computing their inverse is therefore straightforward. Furthermore, when the truncation parameter $\lambda = 0$, $\mathsf{E}^l = \mathsf{E}^r = \mathsf{M}$ and the matrices R and A vanish. Similarly, when the time truncation parameter $s = 0$, $\mathsf{E}^p = \mathsf{N}$.

After these manipulations, we obtain the following set of discrete equations:

$$\mathsf{MFT} = \mathsf{DFP} + \mathsf{Q}, \tag{3.5}$$

where F is the matrix of unknown coefficients and where Q is the reaction matrix whose entries are $\mathsf{Q}_{il} = \langle\!\langle \phi_i^x q(x,t) \phi_l^t \rangle\!\rangle$. To solve (3.5), we shall first recast it in a more convenient form. To do so, we make use of the Kronecker product (represented by $\otimes$) to express (3.5) as

$$\left(\mathsf{T}^T \otimes \mathsf{M} - \mathsf{P}^T \otimes \mathsf{D}\right) \mathrm{vec}(\mathsf{F}) = \mathrm{vec}(\mathsf{Q}), \tag{3.6}$$

where $\mathrm{vec}(\mathsf{F})$ is the vector obtained by stacking the columns of F on top of one another (see the appendix for details) and the superscript T denotes the transpose. It is interesting to note that the matrix approach presented here is very close to Podlubny's matrix approach [32, 33, 34] and could indeed be seen as a generalization to tempered fractional derivatives.

The system matrix in (3.6) is a full $(N_x+1)(N_t+1) \times (N_x+1)(N_t+1)$ matrix. Since the size of that system is generally small thanks to the use of high-order discretization, it can be solved quite quickly using standard approaches. We have therefore only used the standard linear solver available in MATLAB, which is based on a QR decomposition. We have not investigated if more efficient methods like the one proposed by Wang, Wang, and Sircar [40] could be applied to our problem. The total number of operations required for the combined space and time integrations is then $\mathcal{O}((N_x+1)^3(N_t+1)^3)$. As long as the model solution is sufficiently smooth and does not have sharp gradients, such a poor scaling should not be a major issue as the required number of degrees of freedom in space and time would be limited. However, for problems with sharp gradients, a low-order method like the FD or FE method might prove more appropriate.

Equation (3.6) has to be supplemented with the initial and boundary conditions. On the one hand, the initial condition $f(x,0) = f^0(x)$ can be discretized with the Galerkin formulation

$$\langle \phi_i^x \tilde{f}(x,0) \rangle_x = \langle \phi_i^x f^0(x) \rangle_x,$$

and hence

$$\langle \phi_i^x \phi_j^x \rangle_x \, \mathsf{F}_{jk} \phi_k^t(0) = \langle \phi_i^x f^0(x) \rangle_x,$$

where $0 \le i \le N_x$. Since the initial condition does not depend on time, the Galerkin formulation only involves a projection on space basis functions. By using again the properties of the Kronecker product, we can express this set of discrete equations in matrix form as

$$(\mathbf{\Phi}^t(0)^T \otimes \mathbf{M})\mathrm{vec}(\mathbf{F}) = \langle \mathbf{\Phi}^x(x) f^0(x) \rangle_x \ ,$$

where $\mathbf{\Phi}^t(t) = (\phi_0^t(t), \ldots, \phi_{N_t}^t(t))^T$ and $\mathbf{\Phi}^x(x) = (\phi_0^x(x), \ldots, \phi_{N_x}^x(x))^T$. On the other hand, the left boundary condition $c_d^l f(0,t) + c_n^l \frac{\partial f}{\partial x}(0,t) = f^l(t)$ can be discretized as

$$\left\langle \left(c_d^l \tilde{f}(0,t) + c_n^l \frac{\partial \tilde{f}}{\partial x}(0,t) \right) \phi_l^t \right\rangle_t = \langle f^l(t) \phi_l^t \rangle_t$$

and hence

$$\left(c_d^l \phi_j^x(0) + c_n^l \frac{\mathrm{d}\phi_j^x}{\mathrm{d}x}(0) \right) \mathsf{F}_{jk} \ \langle \phi_k^t \phi_l^t \rangle_t = \langle f^l(t) \phi_l^t \rangle_t$$

for $0 \le l \le N_t$. Here we used only a Galerkin formulation in time since the boundary conditions have no explicit dependence on x. We can express the previous set of discrete equations in matrix form as follows:

$$\left(\mathsf{N}^T \otimes \left(c_d^l \mathbf{\Phi}^x(0)^T + c_n^l \frac{\mathrm{d}\mathbf{\Phi}^x}{\mathrm{d}x}(0)^T \right) \right) \mathrm{vec}(\mathbf{F}) = \langle f^l(t) \mathbf{\Phi}^t(t) \rangle_t .$$

The discretization of the right boundary condition, $c_d^r f(L,t) + c_n^r \frac{\partial f}{\partial x}(L,t) = f^r(t)$, is similar.

The N_x+1 discrete equations that represent the initial condition and the $2(N_t+1)$ discrete equations representing the boundary conditions have to be included in the full system of discrete equations. This is achieved by replacing the $N_x + 1$ equations involving the test function $\phi_{N_t}^t$ in (3.6) by the discrete initial condition. Similarly the $2(N_t + 1)$ discrete equations representing the two boundary conditions are included in (3.6) in place of the discrete equations involving the test functions $\phi_{N_x-1}^x$ and $\phi_{N_x}^x$. This approach to impose boundary conditions is called "boundary bordering" by Boyd [3].

4. Numerical results. In this section, we present two numerical examples that highlight the properties of the proposed numerical scheme. In the first example, we assess the convergence rate of the numerical scheme by computing the L_2 relative error with respect to an analytical solution. The second example is more qualitative and shows the diffusion of a Gaussian hill for different values of the parameters α, γ, λ and s.

4.1. Convergence analysis. To evaluate the convergence rate of the proposed PS method, we compute the solution of (2.1) with $\theta = -1$ and the following diffusivity and reaction functions:

$$d(x,t) = x^\alpha \frac{\Gamma(p+1-\alpha)}{\Gamma(p+1)},$$
$$q(x,t) = x^p e^{-\lambda x} e^{-st} \left(q_{\gamma,\beta,s}(t) - t^q q_{\alpha,\lambda}(x) \right),$$

where p and $q \in \mathbb{R}$, and

$$q_{\gamma,\beta,s}(t) = qt^{q-1} - st^q + \beta\frac{\Gamma(q+1)}{\Gamma(q+1-\gamma)}t^{q-\gamma} - \beta s^\gamma t^q,$$
$$q_{\alpha,\lambda}(x) = 1 - \frac{\Gamma(p+1-\alpha)}{\Gamma(p+1)}\left(\lambda^\alpha x^\alpha + \alpha\lambda^{\alpha-1}(px^{\alpha-1} - \lambda x^\alpha)\right).$$

In that case, the exact solution of (2.1) is

$$f(x,t) = x^p t^q e^{-\lambda x} e^{-st}. \tag{4.1}$$

The model equation is solved for $0 \le x \le 1$ and is subject to the following initial and boundary conditions:

$$f(x,0) = f^0(x) = 0,$$
$$f(0,t) = f^l(t) = 0,$$
$$f(1,t) = f^r(t) = t^q e^{-\lambda - st}.$$

The equation has been solved numerically until $t = 1$ with $(\alpha,\gamma) = (1.8, 0.8)$ and $(1.2, 0.2)$, and $\beta = 1$. The truncation parameters λ and s are equal to 0 or 1. We have considered two sets of values for the parameters p and q in (4.1): $(p,q) = (3,3)$ and $(2.8, 2.6)$. The exact solution is therefore $\mathcal{C}^\infty$ when $(p,q) = (3,3)$ but only $\mathcal{C}^2$ when $(p,q) = (2.8, 2.6)$. For each simulation, we take the same number of modes in the space and time expansions, i.e., $N_x = N_t$.

The convergence of the L_2 error is shown in Figure 2. When both p and q are integer, the convergence rate is exponential (left panel of the figure). In the particular case where there is no truncation, the exact solution simply reduces to $f(x,t) = x^p t^q$. The numerical solution is therefore equal to the exact one as soon as $N_x = p + 1$ and $N_t = q + 1$. While numerical results clearly suggest that the proposed method achieves exponential convergence when the solution is smooth, a formal mathematical proof is quite difficult to obtain. The difficulty lies in the fractional-order differential operators that introduce a branch point at $x = 0$ and $t = 0$ when applied to space and time Chebyshev basis functions. That is obviously not the case for classical PDEs and it makes the proof of convergence much more difficult.

When p and q take noninteger values, the solution contains a singularity at $x = 0$ and $t = 0$ and convergence is only algebraic (right panel of Figure 2). According to Darboux's principle, for each type of spectral expansions the rate of convergence is controlled by the strength of the gravest singularity in the complex plane (see [3] for more details). We are, however, not aware of any extension of Darboux's principle to fractional PDEs. Fractional differential operators might also have an effect on the convergence rate as they introduce branch points on the boundaries of the domain. In our example, the fractional time derivative introduces a branch point at $t = 0$ and the fractional space derivative introduces a branch point at $x = 0$. The degree of these singularities depends on the order of the derivatives. We therefore expect the algebraic convergence rate to be influenced both by the gravest singularity in the exact solution and by the orders of the fractional derivatives. In our example, the algebraic convergence rate is close to 3.5 when $(\alpha,\gamma) = (1.2, 0.2)$ and close to 3.7 when $(\alpha,\gamma) = (1.8, 0.8)$.

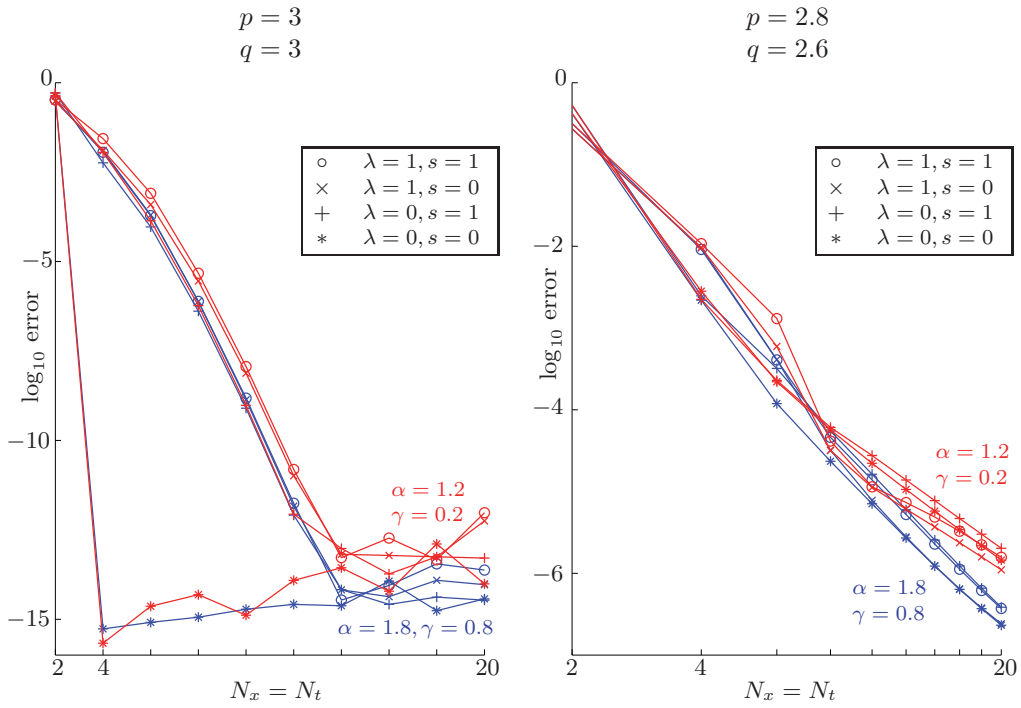

FIG. 2. *Relative L_2 error between the numerical solution of* (2.1) *and the exact solution* $f(x,t) = x^p t^q e^{-\lambda x} e^{-st}$ *with respect to the number of modes in the space* (N_x) *and time* (N_t) *expansions. In this example,* $(\alpha, \gamma) = (1.8, 0.8)$ *and* $(1.2, 0.2)$, $\beta = 1$, $\lambda = 0$ *or* 1, *and* $s = 0$ *or* 1. *The error convergence is exponential when* $p = q = 3$ *as the exact solution is smooth (left panel). However, it is downgraded to an algebraic convergence when* $p = 2.8$ *and* $q = 2.6$ *as the exact solution has a singularity at* $t = 0$ *and* $x = 0$ *(right panel). The algebraic convergence rate is close to* 3.5 *when* $(\alpha, \gamma) = (1.2, 0.2)$ *and close to* 3.7 *when* $(\alpha, \gamma) = (1.8, 0.8)$.

4.2. Diffusion of a Gaussian hill. In this section, we present some numerical solutions of (2.1) for different values of the parameters α, γ, λ, and s and the following initial and boundary conditions:

$$f(x,0) = f^0(x) = \exp(-10(x - L/2)^2),$$
$$\frac{\partial f}{\partial x}(0,t) = f^l(t) = 0,$$
$$f(L,t) = f^r(t) = 0$$

for $L = 10$ and $T = 2$. To account for the change of dimension of the diffusivity and capacity coefficients when changing the values of α and γ, we define them as $d(x,t) = \mathcal{D}\mathcal{L}^\alpha \mathcal{T}^{-1}$ and $\beta = \mathcal{T}^{\gamma - 1}$, where $\mathcal{L}$ and $\mathcal{T}$ are characteristic length and time scale, respectively, and where $\mathcal{D}$ is a dimensionless constant. This amounts to making (2.1) dimensionless with respect to those scales and to taking a dimensionless diffusion coefficient equal to $\mathcal{D}$. For the example presented here, we have selected the following values: $\mathcal{D} = \frac{1}{62.5}$, $\mathcal{L} = \frac{L}{8}$, $\mathcal{T} = \frac{T}{8}$. Because of the steepness of the initial solution, we had to use a Chebyshev polynomial expansion with 190 modes in space. For the time expansion, 10 modes were sufficient. For this example, it could have been more advantageous to use the FD or FE method in space. However, since the goal here is to provide qualitative results showing the evolution of the solution behavior for

different values of the parameters defining the fractional derivatives, the choice of the numerical scheme is less important.

Figure 3 shows the evolution of the solution of (2.1) for different values of α and γ when $\lambda = 0$ and $s = 0$. The classical diffusion pattern with exponentially decaying tails is recovered when $\alpha = 2$ and $\gamma = 1$. A superdiffusive effect is observed when $\alpha < 2$ and $\gamma = 1$. In that case, the diffusion operator is nonlocal and the initially localized solution is quickly spread over the entire domain. A subdiffusive effect is observed when $\alpha = 2$ and $\gamma < 1$. In that case, the solution spreads more slowly and eventually almost freezes. Such a behavior highlights the memory effect that is introduced in the model by replacing the first-order time derivative by a fractional-order derivative of degree less than 1. For the general case where $\alpha < 2$ and $\gamma < 1$, the superdiffusive effect in space competes with the subdiffusive effect in time. The overall behavior of the solution depends on the ratio $\frac{2\gamma}{\alpha}$. For $\frac{2\gamma}{\alpha} > 1$, superdiffusion

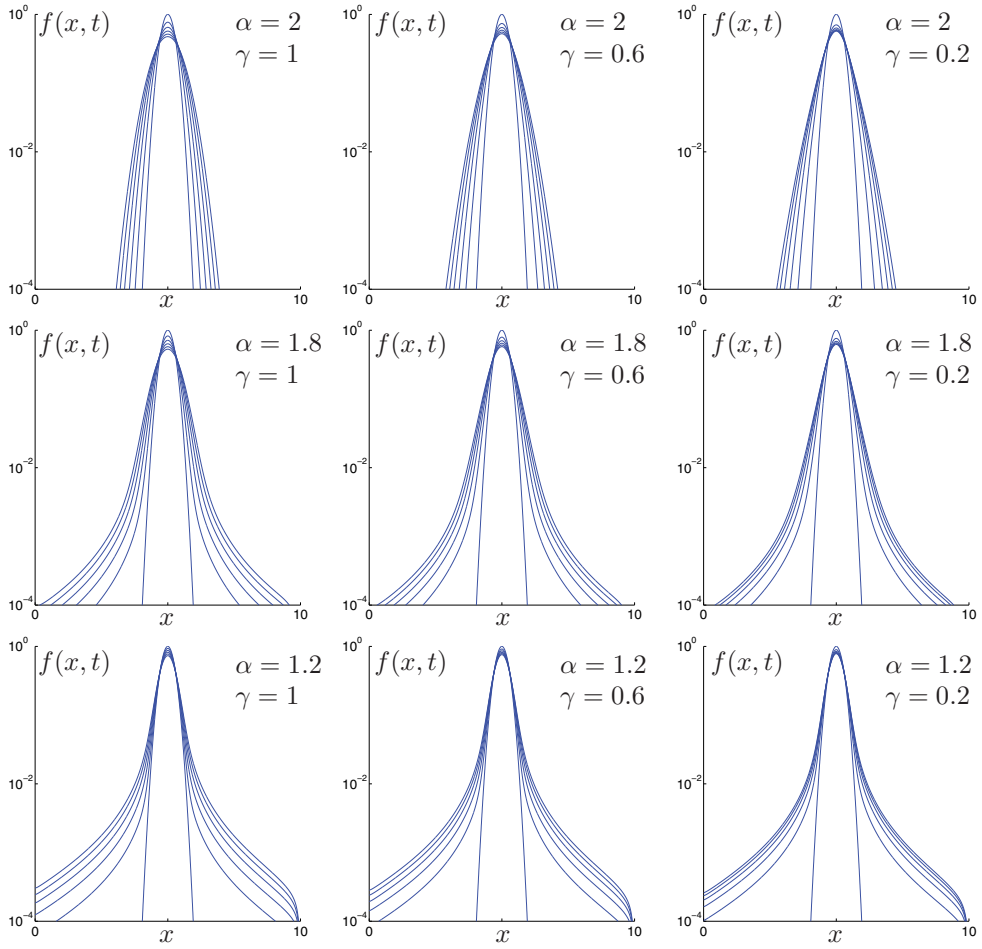

FIG. 3. *Diffusion patterns obtained for different values of α and γ without truncation effects (i.e., $\lambda = s = 0$) at equidistant time instants. Normal diffusion is observed when $\alpha = 2$ and $\gamma = 1$, superdiffusion is observed when $\frac{2\gamma}{\alpha} > 1$, subdiffusion is observed when $\frac{2\gamma}{\alpha} < 1$, and quasi-diffusion is observed when $\frac{2\gamma}{\alpha} = 1$ and $\alpha < 2$. Note that the y-axis is in log scale.*

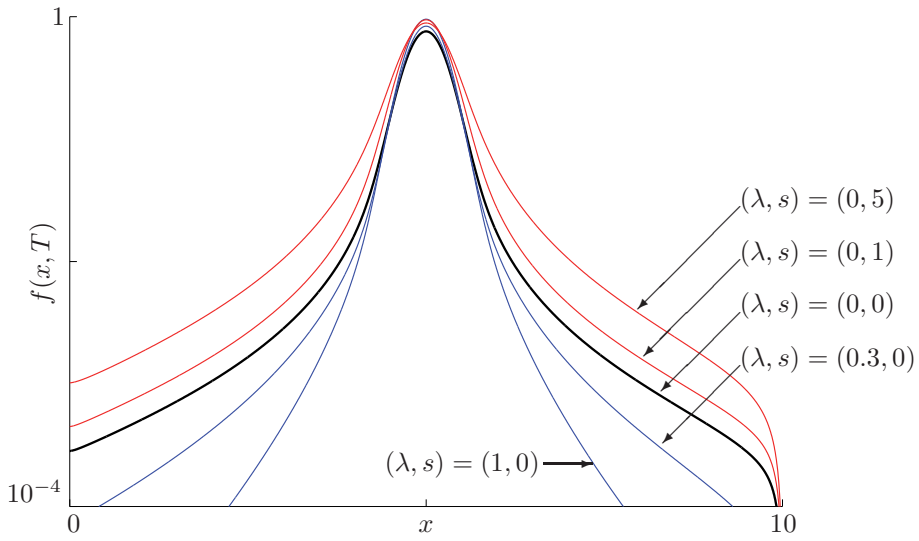

FIG. 4. *Final profiles of the model solution for different values of the pair of truncation parameters* (λ, s) *for* $\alpha = 1.2$ *and* $\gamma = 0.6$. *As the value of* λ *increases, the truncation length decreases and the diffusion process becomes subdiffusive. As the value of* s *increases, the truncation time decreases and the diffusion process becomes superdiffusive. Note that the* y*-axis is in log scale.*

dominates, while subdiffusion dominates for $\frac{2\gamma}{\alpha} < 1$ [27]. When $\frac{2\gamma}{\alpha} = 1$ while $\alpha < 2$ and $\gamma < 1$, the diffusion process is said to be quasi diffusive in the sense that the solution spreads at the same rate as for ordinary diffusion but all its moments are infinite.

Starting from the quasi-diffusive solution corresponding to $\alpha = 1.2$ and $\gamma = 0.6$, we can highlight the effect of the truncation parameters on the solution evolution. By introducing a nonzero truncation effect in space and in time, we reduce the probability of long displacements and long waiting times between displacements. As a result, the quasi-diffusive solution can become superdiffusive when s increases and subdiffusive when λ increases. This behavior is shown qualitatively in Figure 4, where we start from the final solution without truncation (black curve) and vary each of the truncation parameters while keeping the other equal to zero. As expected, the tails of the solution become thicker when s increases (red curves), while they become thinner when λ increases (blue curves).

It should be noted that the model solution does not exactly satisfy the zero-slope boundary condition imposed at $x = 0$. As mentioned at the end of section 2, imposing a vanishing gradient on the boundary does not result in a zero fractional flux on the boundary. Hence the solution slope does not vanish as mass is leaking out of the domain through the boundary. To obtain a zero flux on the boundary, it is necessary to impose a boundary condition that is in agreement with the nonlocal diffusion operator. Such a nonreflecting boundary condition has been derived by Kay et al. in a very recent paper [15]. We leave the investigation of such boundary conditions in a PS model to a future study.

5. Conclusions. In this work, we have derived a PS scheme based on a Chebyshev expansion in space and time to solve the fractional diffusion equation. Both the space and time fractional derivatives have been tempered to account for the finite limits of the physical domain. The resulting model is applicable to a wide range

of realistic systems that show a slow transition from anomalous to asymptotic normal diffusion over time.

By expanding the model solution in terms of Chebyshev polynomials in both space and time, we were able to derive a high-order scheme that easily accommodates tempered fractional-order differential operators. All the calculations can be performed analytically or numerically with an arbitrarily large degree of accuracy. As a result, an accurate solution can be obtained with a relatively small number of degrees of freedom and hence at a reasonable computational cost.

It should be pointed out that the proposed method to discretize the model equation could also accommodate other numerical methods. For instance, if the model solution is not smooth in space, the PS scheme can suffer from the Runge phenomenon. That could be prevented by simply replacing the Chebyshev basis functions in space by low-order FE basis functions or radial basis functions and deriving the corresponding mass and diffusion matrices by following the same procedure as the one described in this study.

Appendix. Kronecker product. If we consider the matrices $\mathsf{A} \in \mathbb{R}^{m\times n}$ and $\mathsf{B} \in \mathbb{R}^{p\times q}$, then the Kronecker product of A and B is defined as the matrix

$$\mathsf{A}\otimes\mathsf{B} = \begin{bmatrix} a_{11}\mathsf{B} & \dots & a_{1n}\mathsf{B} \\ \vdots & \ddots & \vdots \\ a_{m1}\mathsf{B} & \dots & a_{mn}\mathsf{B} \end{bmatrix} \in \mathbb{R}^{mp\times nq}.$$

The Kronecker product has the useful property that for any three matrices A, B, and C for which the matrix product is defined, we have

$$\mathrm{vec}(\mathsf{ABC}) = (\mathsf{C}^T \otimes \mathsf{A})\mathrm{vec}(\mathsf{B}), \tag{A.1}$$

where $\mathrm{vec}(\mathsf{B})$ is the vector obtained by stacking the columns of B on top of one another [19].

Acknowledgments. Part of the research was carried out at the Department of Information Technology, Uppsala University, Sweden, under a visiting researcher program. The implementation of the numerical method presented in this paper has been made much easier thanks to the use of the Chebfun library [38].

REFERENCES

[1] B. Baeumer and M. M. Meerschaert, *Tempered stable Lévy motion and transient superdiffusion*, J. Comput. Appl. Math., 233 (2010), pp. 2438–2448.
[2] D. A. Benson, M. M. Meerschaert, and J. Revielle, *Fractional calculus in hydrologic modeling: A numerical perspective*, Adv. Water Resources, 51 (2013), pp. 479–497.
[3] J. P. Boyd, *Chebyshev and Fourier Spectral Methods*, 2nd ed., Dover Publications, New York, 2001.
[4] A. R. Carella and C. A. Dorao, *Least-squares spectral method for the solution of a fractional advection-dispersion equation*, J. Comput. Phys., 232 (2013), pp. 33–45.
[5] A. Cartea and D. del Castillo Negrete, *Fluid limit of the continuous-time random walk with general Lévy jump distribution functions*, Phys. Rev. E, 76 (2007), 041105.
[6] A Cartea and D. del Castillo Negrete, *Fractional diffusion models of option prices in markets with jumps*, Phys. A, 374 (2007), pp. 749–763.
[7] M. Cui, *Compact alternating direction implicit method for two-dimensional time fractional diffusion equation*, J. Comput. Phys., 231 (2012), pp. 2621–2633.
[8] D. del Castillo Negrete, *Truncation effects in superdiffusive front propagation with Lévy flights*, Phys. Rev. E, 79 (2009), pp. 1–10.

[9] E. H. Doha, A. H. Bhrawy, and S. S. Ezz-Eldien, *Efficient Chebyshev spectral methods for solving multi-term fractional orders differential equations*, Appl. Math. Model., 35 (2011), pp. 5662–5672.
[10] S. Esmaeili and M. Shamsi, *A pseudo-spectral scheme for the approximate solution of a family of fractional differential equations*, Commun. Nonlinear Sci. Numer. Simul., 16 (2011), pp. 3646–3654.
[11] G. J. Fix and J. P. Roop, *Least square finite-element solution of a fractional order two-point boundary value problem*, Comput. Math. Appl., 48 (2004), pp. 1017–1033.
[12] E. Hanert, *A comparison of three Eulerian numerical methods for fractional-order transport models*, Environ. Fluid Mech., 10 (2010), pp. 7–20.
[13] E. Hanert, *On the numerical solution of space-time fractional diffusion models*, Comput. Fluids, 46 (2011), pp. 33–39.
[14] Q. Huang, G. Huang, and H. Zhan, *A finite element solution for the fractional advection-dispersion equation*, Adv. Water Resources, 31 (2008), pp. 1578–1589.
[15] D. Kay, I. Turner, N. Cusimano, and K. Burrage, *Reflections from a boundary: Reflecting boundary conditions for space-fractional partial differential equations on bounded domains*, submitted.
[16] I. Koponen, *Analytic approach to the problem of convergence of truncated Lévy flights towards the Gaussian stochastic process*, Phys. Rev. E, 52 (1995), pp. 1197–1199.
[17] N. Krepysheva, L. Di Pietro, and M.-C. Neel, *Space-fractional advection-diffusion and reflective boundary conditions*, Phys. Rev. E, 73 (2006), 021104.
[18] A. Kullberg and D. del Castillo-Negrete, *Transport in the spatially tempered, fractional Fokker-Planck equation*, J. Phys. A, 45 (2012).
[19] A. J. Laub, *Matrix Analysis for Scientists and Engineers*, SIAM, Philadelphia, 2005.
[20] C. Li, F. Zeng, and F. Liu, *Spectral approximations to the fractional integral and derivative*, Fract. Calc. Appl. Anal., 15 (2012), pp. 383–406.
[21] X. Li and C. Xu, *A space-time spectral method for the time fractional diffusion equation*, SIAM J. Numer. Anal., 47 (2009), pp. 2108–2131.
[22] Y. Lin and C. Xu, *Finite difference/spectral approximations for the time-fractional diffusion equation*, J. Comput. Phys., 225 (2007), pp. 1533–1552.
[23] R. N. Mantegna and H. E. Stanley, *Stochastic process with ultraslow convergence to a Gaussian: The truncated Lévy flight*, Phys. Rev. Lett., 73 (1994), pp. 2946–2949.
[24] M. M. Meerschaert and C. Tadjeran, *Finite difference approximations for fractional advection-diffusion flow equations*, J. Comput. Appl. Math., 172 (2004), pp. 65–77.
[25] M. M. Meerschaert and C. Tadjeran, *Finite difference approximations for two-sided space-fractional partial differential equations*, Appl. Numer. Math., 56 (2006), pp. 80–90.
[26] M. M. Meerschaert, Y. Zhang, and B. Baeumer, *Tempered anomalous diffusion in heterogeneous systems*, Geophys. Res. Lett., 35 (2008).
[27] R. Metzler and J. Klafter, *The random walk's guide to anomalous diffusion: A fractional dynamics approach*, Phys. Rep., 339 (2000), pp. 1–77.
[28] R. Metzler and J. Klafter, *The restaurant at the end of the random walk: Recent development in the description of anomalous transport by fractional dynamics*, J. Phys. A, 37 (2004), pp. 161–208.
[29] H.-K. Pang and H.-W. Sun, *Multigrid method for fractional diffusion equations*, J. Comput. Phys., 231 (2012), pp. 693–703.
[30] C. Piret and E. Hanert, *A radial basis functions method for fractional diffusion equations*, J. Comput. Phys., 238 (2013), pp. 71–81.
[31] I. Podlubny, *Fractional Differential Equations*, Math. Sci. Engrg. 198, Academic Press, New York, 1999.
[32] I. Podlubny, *Matrix approach to discrete fractional calculus*, Fract. Calc. Appl. Anal., 3 (2000), pp. 359–386.
[33] I. Podlubny, A. Chechkin, T. Skovranek, Y. Chen, and B. M. Vinagre Jara, *Matrix approach to discrete fractional calculus II: Partial fractional differential equations*, J. Comput. Phys., 228 (2009), pp. 3137–3153.
[34] I. Podlubny, T. Skovranek, B. M. Vinagre Jara, I. Petras, V. Verbitsky, and Y. Q. Chen, *Matrix approach to discrete fractional calculus* III*: Non-equidistant grids, variable step length and distributed orders*, Philos. Trans. R. Soc. A Math., Phys. Engrg. Sci., 371 (2013).
[35] J. P. Roop, *Computational aspects of FEM approximation of fractional advection dispersion equations on bounded domains in* $\mathbb{R}^2$, J. Comput. Appl. Math., 193 (2006), pp. 243–268.
[36] J. Rosiński, *Tempering stable processes*, Stochastic Process. Appl., 117 (2007), pp. 677–707.

[37] C. Tadjeran, M. M. Meerschaert, and H.-P. Scheffler, *A second-order accurate numerical approximation for the fractional diffusion equation*, J. Comput. Phys., 213 (2006), pp. 205–213.
[38] L. N. Trefethen et al., *Chebfun Version* 4.0, Chebfun Development Team, http://www.maths.ox.ac.uk/chebfun (2011).
[39] H. Wang and K. Wang, *A direct $O(Nlog^2N)$ alternating-direction finite difference method for two-dimensional fractional diffusion equations*, J. Comput. Phys., 230 (2011), pp. 7830–7839.
[40] H. Wang, K. Wang, and T. Sircar, *A direct $O(Nlog^2N)$ finite difference method for fractional diffusion equations*, J. Comput. Phys., 229 (2010), pp. 8095–8104.
[41] M. Zayernouri and G. E. Karniadakis, *Fractional spectral collocation method*, SIAM J. Sci. Comput., 36 (2014), pp. 40–62.
[42] X. Zhang, M. Lv, J. W. Crawford, and I. M. Young, *The impact of boundary on the fractional advection-dispersion equation for solute transport in soil: Defining the fractional dispersive flux with the caputo derivatives*, Adv. Water Resources, 30 (2007), pp. 1205–1217.
[43] Y. Zhang, *Moments for tempered fractional advection-diffusion equations*, J. Statist. Phys., 139 (2010), pp. 915–939.
[44] Y. Zhang, B. Baeumer, and D. M. Reeves, *A tempered multiscaling stable model to simulate transport in regional-scale fractured media*, Geophys. Res. Lett., 37 (2010).
[45] Y. Zhang and C. Papelis, *Particle-tracking simulation of fractional diffusion-reaction processes*, Phys. Rev. E, 84 (2011).